Inorganic Chemistry

Article

pubs.acs.org/IC

Luminescent Hydrogel Particles Prepared by Self-Assembly of β-Cyclodextrin Polymer and Octahedral Molybdenum Cluster Complexes

Kaplan Kirakci,*[,†] Václav Šícha,[†] Josef Holub,[†] Pavel Kubát,[‡] and Kamil Lang*[,†]

[†]Institute of Inorganic Chemistry of the AS CR, v.v.i, Husinec-Řež 1001, 250 68 Řež, Czech Republic

[‡]J. Heyrovský Institute of Physical Chemistry of the AS CR, v.v.i, Dolejškova 3, 182 23 Praha 8, Czech Republic

Supporting Information

ABSTRACT: A series of luminescent octahedral molybdenum cluster complexes were obtained by treating $Na_2[Mo_6I_8(OMe)_6]$ with icosahedral *closo*-dicarbaborane C-carboxylic acids in refluxing tetrahydrofuran. The study of the photophysical properties of $Na_2[Mo_6I_8(1\text{-}OOC\text{-}1,2\text{-}closo\text{-}C_2B_{10}H_{11})_6]$ (**1**), $Na_2[Mo_6I_8(1\text{-}OOC\text{-}1,7\text{-}closo\text{-}C_2B_{10}H_{11})_6]$ (**2**), and $Na_2[Mo_6I_8(1\text{-}OOC\text{-}1,12\text{-}closo\text{-}C_2B_{10}H_{11})_6]$ (**3**) in acetonitrile revealed a red luminescence with high quantum yields up to 0.93 for **2**, an efficient quenching of the luminescence by oxygen, and high quantum yields of singlet oxygen formation of approximately 0.7. Self-assembly between compound **2** and β-cyclodextrin polymer led to monodisperse hydrogel particles with a diameter of approximately 200 nm and unchanged luminescence spectra and kinetics features over 14 days. In contrast, bare cluster complex **2** in water formed aggregates and hydrolyzed over the time as indicated by a progressive red shift of the luminescence maxima. The invariance of key photophysical parameters of the hydrogel particles coupled with a high oxygen sensitivity of the luminescence are attractive features for long-term biological experiments involving optical oxygen probing. In addition, this hydrogel is a singlet oxygen sensitizer in water with promising properties for photodynamic therapy.

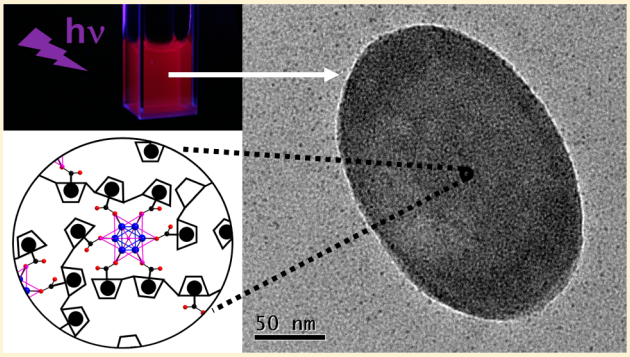

INTRODUCTION

Among the variety of phosphorescent dyes, the octahedral molybdenum cluster complexes $[Mo_6L_{14}]^{2-}$ have recently emerged as relevant building blocks for the construction of photofunctional materials thanks to promising photophysical properties and simple synthetic protocols. Upon excitation from the UV to green spectral regions, they form long-lived triplet states that relax via a red luminescence with quantum efficiencies close to 100%.[1] Their luminescence is quenched by molecular oxygen forming the reactive singlet oxygen, $O_2(^1\Delta_g)$, with quantum yields up to 0.92.[2,3] Such properties have already been exploited in various functional materials such as optical oxygen sensors,[4] light convertors for photovoltaics,[5] or photocatalysts.[6] The $[Mo_6L_{14}]^{2-}$ cluster complexes are constructed from an octahedron of molybdenum atoms (Mo^{II}) surrounded by eight face-capping halogen and six inorganic or organic apical ligands. The photophysical properties are strongly affected by the nature of ligands. In this respect, the coordination of carboxylates to the $\{Mo_6I_8\}^{4+}$ core can lead to desired intrinsic properties in terms of luminescence efficiency, oxygen sensing ability, and singlet oxygen production.[3,7] In addition, the use of carboxylates as apical ligands allows for an additional functionalization of the clusters providing the propensity to form liquid crystals via mesogenic ligands,[8] an increased absorption and the antenna effect,[9] or the ability to copolymerize with methacrylate monomers.[10]

The low stability of molybdenum clusters in water at physiological pH remains a barrier for biological applications such as oxygen probing or singlet oxygen sensitization. Indeed, the archetypal molybdenum halides $[Mo_6X_{14}]^{2-}$ (X = Cl, Br, and I) are known to be stable only in concentrated aqueous solutions of their related acid HX and an increase of the pH causes the formation of aqua-hydroxo complexes $[Mo_6X_x(OH)_y(H_2O)_z]^n$.[11] From a practical point of view, this hydrolysis is detrimental as it leads to microsized aggregates with poorly defined photophysical properties. In addition, such aggregates have shown an acute toxicity for living organisms, which restricts the use of cluster complexes in biological applications.[11] These difficulties have been overcome by the embedding of cluster complexes in silica nanoparticles or in polystyrene beads, which have shown promising results for luminescent probing or singlet oxygen sensitization.[1,12,13] The methods used to date are based on the covalent binding of the complexes to a corresponding matrix and causes the changes in photophysical properties, thus limiting the control over them.

Received: September 3, 2014
Published: November 24, 2014

   dx.doi.org/10.1021/ic502144z | Inorg. Chem. 2014, 53, 13012−13018

An unexplored approach lies in the grafting of hydrophobic apical ligands capable of forming inclusion complexes with container macrocycles that provide a protection against the hydrolysis and ensure a good dispersibility in water without affecting the photophysical properties of the cluster. Cyclodextrin derivatives are cyclic oligosaccharides made of glucopyranose units arranged in a truncated cone. The interior of the cavity, which is lined with C−H groups and glycosidic oxygen bridges, is hydrophobic, whereas the exterior is hydrophilic due to the presence of hydroxyl groups. Because of their low toxicity, cyclodextrin derivatives can be used in living organisms as carriers of hydrophobic drugs or luminescent probes.[14−16] In addition, self-assembly of polymeric cyclodextrin and hydrophobic moieties allows for the construction of biomaterials such as hydrogels, nanoassemblies, and biomatrices.[17,18] Among possible guests with β-cyclodextrin polymers, C-substituted carboxylates of icosahedral *closo*-dicarbaboranes with large affinities toward β-cyclodextrin derivatives[19−21] were chosen in this work as hydrophobic apical ligands grafted to the $\{Mo_6I_8\}^{4+}$ core. Carboranes are electron delocalized polyhedral borane clusters with one or more boron vertices substituted with carbon atoms. Among the carborane clusters, the icosahedral *closo*-dicarbaboranes of the general formula $C_2B_{10}H_{12}$ are of high interest due to their remarkable chemical, physical, and biological properties (i.e., stability, hydrophobicity, 3D shape, aromaticity) and broad possibilities for their exoskeletal modification of each boron and carbon atom.[22]

In this Article, we report the preparation and characterization of luminescent hydrogel particles prepared by self-assembly between polymeric β-cyclodextrins and new octahedral molybdenum cluster complexes with icosahedral *closo*-dicarbaborane C-carboxylates as apical ligands. The photophysical properties of $Na_2[Mo_6I_8(1\text{-}OOC\text{-}1,2\text{-}closo\text{-}C_2B_{10}H_{11})_6]$ (**1**), $Na_2[Mo_6I_8(1\text{-}OOC\text{-}1,7\text{-}closo\text{-}C_2B_{10}H_{11})_6]$ (**2**), and $Na_2[Mo_6I_8(1\text{-}OOC\text{-}1,12\text{-}closo\text{-}C_2B_{10}H_{11})_6]$ (**3**) (Figure 1) in acetonitrile were studied by absorption and luminescence spectroscopy. The morphology and stability of the luminescent hydrogel based on compound **2** and polymeric β-cyclodextrin (**2@poly-β-CD**) were evaluated in detail and compared with those of water dispersion of **2**.

EXPERIMENTAL SECTION

Caution. $Na_2[Mo_6I_8(OMe)_6]$ is strongly basic and should be handled with appropriate protections.

Reagents. Starting compounds [1-HOOC-1,2-*closo*-$C_2B_{10}H_{11}$], [1-HOOC-1,7-*closo*-$C_2B_{10}H_{11}$], [1-HOOC-1,12-*closo*-$C_2B_{10}H_{11}$], $Na_2[Mo_6I_8(OMe)_6]$, and compounds **1**−**3** were prepared by the methods derived from previously published procedures.[9,23] All chemicals were obtained from Sigma-Aldrich and used as received, except the precursors for icosahedral dicarbaboranes, which were purchased from Katchem (Czech Republic). β-Cyclodextrin polymer had an average molecular weight of 2000−300 000 Da and a mass content of β-cyclodextrin of 60%. Solvents for syntheses were purchased from Penta (Czech Republic), dried, and degassed before use by standard methods. Where necessary, manipulations were performed under an inert atmosphere using a Schlenk line.

Instrumental Techniques. NMR spectra were recorded at 400 MHz (^{1}H) and 128 MHz (^{11}B) using a Varian Mercury 400Plus spectrometer. The assignment of δ (^{1}H{^{11}B}) shifts was based on selectively decoupled δ(^{1}H)-{^{11}B selective}NMR experiments. Coupling constants $^1J(^{11}B-^1H)$ were measured by resolution-enhanced ^{11}B NMR spectra with a digital resolution of 2 Hz. The ^{11}B NMR assignment is based on {^{11}B−^{11}B} COSY NMR spectroscopy.

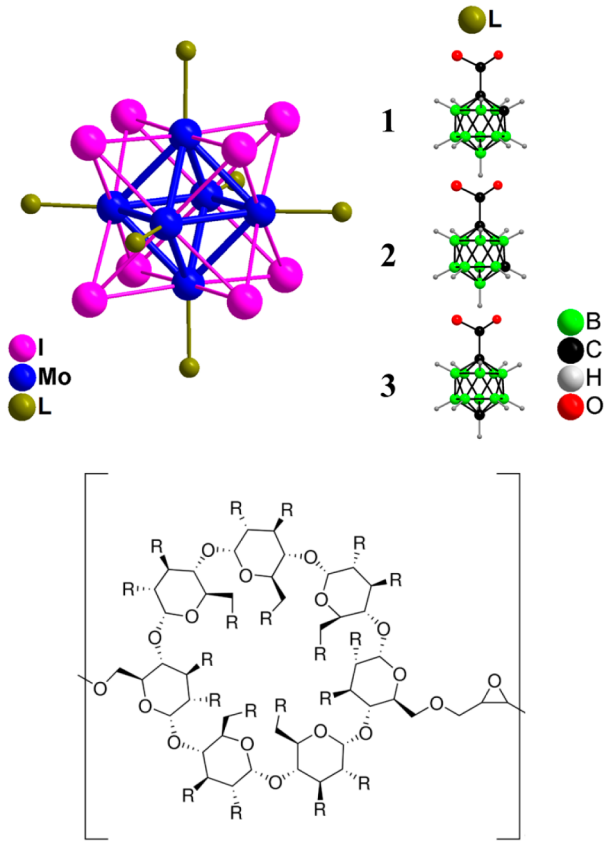

Figure 1. Schematic structures of the studied cluster complexes $Na_2[Mo_6I_8(1\text{-}OOC\text{-}1,2\text{-}closo\text{-}C_2B_{10}H_{11})_6]$ (**1**), $Na_2[Mo_6I_8(1\text{-}OOC\text{-}1,7\text{-}closo\text{-}C_2B_{10}H_{11})_6]$ (**2**), $Na_2[Mo_6I_8(1\text{-}OOC\text{-}1,12\text{-}closo\text{-}C_2B_{10}H_{11})_6]$ (**3**), and β-cyclodextrin polymer.

Elemental analysis was performed on a PerkinElmer CHN/S Elemental analyzer 2400 II. Mass spectrometry measurements were performed on a Thermo Scientific LCQ Fleet Ion Trap instrument using electrospray (ESI) ionization with helium (5.0 Messer, Czech Republic) as a collision gas in the ion trap. The size of particles in water was determined on a particle size analyzer Zetasizer Nano ZS from Malvern (United Kingdom). The size and morphology were also characterized by high-resolution transmission electron microscopy (HRTEM) using a JEM-3010 (JEOL, Japan) operating at 300 kV and probed by molybdenum and iodine mappings using an EDX detector (Oxford Instruments, United Kingdom). The samples for HRTEM were spread on a carbon-coated copper grid. Atomic force microscopy (AFM) images were collected on a Bruker Dimension Icon in Scanasyst mode using Scanasystair cantilevers (a silicon tip on a silicon nitride lever). The samples were prepared by spin-coating on a mica surface. Absorption spectra were recorded on a PerkinElmer Lambda 35 spectrometer. FTIR spectra were recorded using a Nicolet Nexus 670-FT spectrometer in pressed KBr pellets.

Corrected luminescence spectra were monitored on a Fluorolog 3 spectrometer (Horiba Jobin Yvon) with a cooled TBX-05-C photon detection module. The same instrument was used for luminescence lifetime experiments using an excitation at 390 nm (SpectraLED-390). The decay curves were fitted to exponential functions by the iterative reconvolution procedure of the DAS6 software (v 6.4, Horiba Jobin Yvon, 2009). The luminescence spectra of $O_2(^1\Delta_g)$ were detected using a Hamamatsu H10330-45 photomultiplier with the excitation wavelengths between 350 and 500 nm. The luminescence quantum yields, Φ_L, in oxygen-free acetonitrile solutions were measured by the comparative method with $(n\text{-}Bu_4N)_2[Mo_6Cl_{14}]$ (λ_{exc} = 440 nm, Φ_L = 0.15 in oxygen-free acetonitrile)[3] as a reference. All solutions had absorption below 0.05 (for a 10 mm cell) at the excitation wavelength

dx.doi.org/10.1021/ic502144z | Inorg. Chem. 2014, 53, 13012−13018

of 440 nm. The results are the means of three independent experiments. The quantum yields were calculated using

$$\Phi_L = \Phi_L^R \left(\frac{\text{Area}}{\text{Area}^R} \right)$$

where the superscript R corresponds to the reference and Area is the integrated emission intensity normalized to corresponding absorbance. The estimated error was 10%.

Laser flash photolysis experiments were performed with a Lambda Physik COMPEX 102 excimer laser (λ_{exc} = 308 nm, fwhm 28 ns) or a Lambda Physik FL3002 dye laser (λ_{exc} = 425 nm). The transient absorption and luminescence traces were measured using a LKS 20 laser kinetic spectrometer (Applied Photophysics, UK) equipped with a 150 W Xe lamp, pulse unit, and R928 photomultiplier (Hamamatsu). Where appropriate, the samples were saturated by oxygen and argon. The oxygen solubility of 2.42×10^{-3} M in air-saturated acetonitrile was used for calculation of oxygen quenching constants.[24] Time-resolved near-infrared luminescence of $O_2(^1\Delta_g)$ at 1270 nm was observed at a right angle to the excitation light (λ_{exc} = 308 nm) using a homemade detector unit (interference filter, Ge diode). The quantum yields of $O_2(^1\Delta_g)$ formation, Φ_Δ, were estimated by the comparative method using anthracene as a standard ($\Phi_\Delta = 0.69 \pm 0.02$ in oxygen-saturated acetonitrile).[25] Incident energy was used within the energy region where the intensity of a luminescence signal is directly proportional to the incident energy (i.e., less than 2 mJ).

Synthesis of $Na_2[Mo_6I_8(1\text{-}OOC\text{-}1,2\text{-}closo\text{-}C_2B_{10}H_{11})_6]$ (1). A mixture of $Na_2[Mo_6I_8(OMe)_6]$ (100 mg, 58 μmol) and 1-HOOC-1,2-*closo*-$C_2B_{10}H_{11}$ (58 mg, 348 μmol) in 5 mL of tetrahydrofuran (THF) was heated at reflux under an inert atmosphere for 3 days. The resulting mixture was filtered, evaporated to dryness, and washed 3 times by 20 mL of dichloromethane in order to remove unreacted 1-HOOC-1,2-*closo*-$C_2B_{10}H_{11}$, yielding an orange powder that was dried under reduced pressure. The yield was 87%. Anal. Calcd for $C_{18}H_{66}B_{60}I_8Mo_6O_{12}Na_2$: C, 7.83, H, 2.41, Found: C, 7.56, H, 2.27; melting point above 350 °C (decomposition); ^{11}B NMR (128 MHz; THF-d_8; $Et_2O{\cdot}BF_3$) δ_B/ppm: −4.29 (d, 2B, J = 140 Hz, B(9,12)H), −10.52 (d, 2B, J = 150 Hz, B(8,10)H), −12.85 (d, 6B, J = 299 Hz, B(3,4,5,6,7,11)H); ^{1}H NMR (400 MHz; THF-d_8; Me_4Si) δ_H/ppm: 4.46 (s, 1H, C(2)H), 2.34 (s, 6H, B(3,4,5,6,7,11)H), 2.26 (s, 2H, B(9,12)H), 2.12 (s, 2H, B(8,10)H); ESI-MS m/z: 1357.42, calcd. 1357.36 $[M]^{2-}$; UV−vis (acetonitrile): λ_{max}/nm (ε/M^{-1} cm^{-1}) = 295 (1.22×10^4), 338 (7.4×10^3), 395 (5.5×10^3).

Synthesis of $Na_2[Mo_6I_8(1\text{-}OOC\text{-}1,7\text{-}closo\text{-}C_2B_{10}H_{11})_6]$ (2). The same protocol as above except with [1-HOOC-1,7-*closo*-$C_2B_{10}H_{11}$]. The yield was 91%. Anal. Calcd for $C_{18}H_{66}B_{60}I_8Mo_6O_{12}Na_2$: Calc. C, 7.83, H, 2.41, Found: C, 7.68, H, 2.45; melting point above 350 °C (decomposition); ^{11}B NMR (128 MHz; THF-d_8; $Et_2O{\cdot}BF_3$) δ_B/ppm: −6.05 (d, 1B, J = 128 Hz, B(5)H), −12.09 (d, 5B, J = 146 Hz, B(8,9,10,11,12)H), −14.47 (d, 2B, J = 174 Hz, B(4,6)H), −16.30 (d, 2B, J = 226 Hz, B(2,3)H); ^{1}H NMR (400 MHz; THF-d_8; Me_4Si) δ_H/ppm: 3.57 (s, 1H, C(7)H), 2.88 (s, 2H, B(2,3)H), 2.53 (s, 1H, B(5)H), 2.38 (s, 2H, B(8,10)H), 2.16 (s, 3H, B(4,6,11)H), 2.07 (s, 2H, B(9,12)H); ESI-MS m/z: 1357.44, calcd. 1357.36 $[M]^{2-}$; UV−vis (acetonitrile): λ_{max}/nm (ε/M^{-1} cm^{-1}) = 295 (1.24×10^4), 341 (7.3×10^3), 395 (5.4×10^3).

Synthesis of $Na_2[Mo_6I_8(1\text{-}OOC\text{-}1,12\text{-}closo\text{-}C_2B_{10}H_{11})_6]$ (3). The same protocol as above except with [1-HOOC-1,12-*closo*-$C_2B_{10}H_{11}$]. The yield was 89%. Anal. Calcd for $C_{18}H_{66}B_{60}I_8Mo_6O_{12}Na_2$: C, 7.83, H, 2.41, Found: C, 8.15, H, 2.12; melting point above 350 °C (decomposition); ^{11}B NMR (128 MHz; THF-d_8; $Et_2O{\cdot}BF_3$) δ_B/ppm: −14.09 (d, 5B, J = 165 Hz, B(2,3,4,5,6)H), −16.34 (d, 5B, J = 168 Hz, B(7,8,9,10,11)H); ^{1}H NMR (400 MHz; THF-d_8; Me_4Si) δ_H/ppm: 3.62 (s, 1H, C(12)H), 2.48−2.37 (br s, 5H, B(2,3,4,5,6)H), 2.13−2.08 (br s, 5H, B(7,8,9,10,11)H); ESI-MS m/z: 1357.39, calcd. 1357.36 $[M]^{2-}$; UV−vis (acetonitrile): λ_{max}/nm (ε/M^{-1} cm^{-1}) = 295 (1.23×10^4), 339 (7.9×10^3), 395 (6.0×10^3).

Preparation of 2@poly-β-CD. All procedures were carried out at room temperature. Compound **2** (2 mg, 0.72 μmol) was dissolved in THF (20 mL) and the resulting solution was added to a dispersion of β-cyclodextrin polymer (10 mg, equivalent to ∼5.3 μmol of β-cyclodextrin) in deionized water (20 mL). The mixture was sonicated for 15 min and THF was completely removed on a rotary evaporator. The resulting dispersion was filtrated and the volume was readjusted to 20 mL with deionized water. Dispersions used for the measurement of $O_2(^1\Delta_g)$ were prepared in D_2O instead of deionized water.

Preparation of Water Dispersion of 2. The same protocol developed for **2@poly-β-CD** was applied on bare **2**.

RESULTS AND DISCUSSION

Synthesis and Characterization of Title Complexes 1−3. Compounds $Na_2[Mo_6I_8(1\text{-}OOC\text{-}1,2\text{-}closo\text{-}C_2B_{10}H_{11})_6]$ (**1**), $Na_2[Mo_6I_8(1\text{-}OOC\text{-}1,7\text{-}closo\text{-}C_2B_{10}H_{11})_6]$ (**2**), and $Na_2[Mo_6I_8(1\text{-}OOC\text{-}1,12\text{-}closo\text{-}C_2B_{10}H_{11})_6]$ (**3**) (Figure 1) were obtained in high yields by the reaction of $Na_2[Mo_6I_8(OMe)_6]$ with the corresponding *closo*-dicarbaborane C-carboxylic acids in refluxing tetrahydrofuran for 3 days. The formation of the products was monitored by ^{1}H and ^{11}B NMR measurements in d_8-THF (Experimental Section and Figures S1−S39 in the Supporting Information). The disappearance of the ^{1}H signals of the COOH protons of starting acids was in accordance with the coordination of dicarbaboranes to the $\{Mo_6I_8\}^{4+}$ core through their carboxylate functions. When compared with the starting carboxylic acids, the ^{1}H NMR signals of the CH protons of **1−3** exhibited upfield shifts of 0.39, 0.16, and 0.20 ppm, respectively. The BH protons were little influenced by the coordination and the shifts were lower than 0.14 ppm, apart for the ^{1}H NMR signal of B(12)H in **2** with an upfield shift of 0.24 ppm. After conjugation with the molybdenum core, the ^{11}B NMR peaks were broadened and overlapped, especially in the case of **1**. Apart from the ^{11}B NMR signals of B(3) and B(6) that were only weakly influenced by the coordination, the other ^{11}B signals in **1−3** showed upfield shifts ranging between 1.93 ppm for equivalent B(2), B(3), B(4), B(5), and B(6) in **3** and 5.90 ppm for B(12) for **2**. Overall, the strongest shifts of the NMR signals upon coordination were observed for the lowest symmetry isomer. The broadening of the ^{11}B NMR peaks can be attributed to coupling with the nuclear momentum of molybdenum atoms. The ESI mass spectra of **1−3** in acetonitrile revealed peaks of double-charged anionic species with m/z ratios corresponding to $[Mo_6I_8(OOCC_2B_{10}H_{11})_6]^{2-}$ (Figures S40−S42 in the Supporting Information). C and H elemental analysis confirmed the purity of the bulk material used for the measurement of the photophysical properties.

Photophysical Properties of 1−3. As shown in Figure 2, acetonitrile solutions of **1−3** had absorption spectra with broad bands extending from the UV up to 500 nm. The broad maxima were the same with higher molar absorption coefficients when compared to the relevant cluster complex with the ligands bound via carboxylates, i.e., $(n\text{-}Bu_4N)_2[Mo_6I_8(OOCCF_3)_6]$ (compare $\varepsilon_{340} = 5.0 \times 10^3$ M^{-1} cm^{-1} with $\varepsilon_{340} = 7.4 \times 10^3$ M^{-1} cm^{-1} for **1**, both in acetonitrile).[1] Figure 2 also shows the normalized luminescence spectra of **1−3**. All studied cluster complexes exhibited the same broad luminescence band with maxima at 685 nm indicating that differences in the dipole moments of the respective carborane isomers do not affect the energies of the radiative transitions. The asymmetric structure of these bands with a long tail in the near-IR region are characteristic of the $[Mo_6I_8(OOC\text{-}R)_6]^{2-}$ cluster complexes.[1,7,9] The photophysical properties are summarized in Table 1.

dx.doi.org/10.1021/ic502144z | Inorg. Chem. 2014, 53, 13012−13018

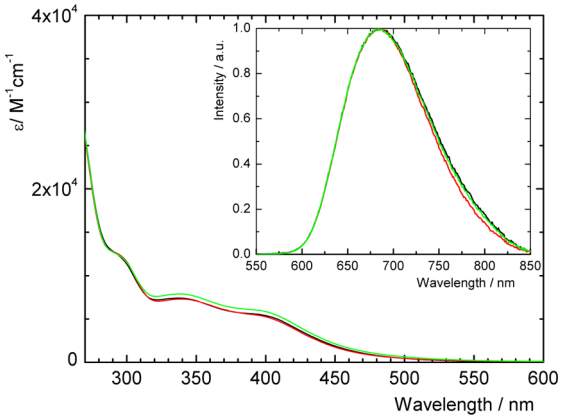

Figure 2. Absorption spectra of **1** (black), **2** (red), and **3** (green) in acetonitrile. Inset: Normalized emission spectra of **1**, **2**, and **3** upon excitation at 440 nm in deoxygenated acetonitrile.

Table 1. Photophysical Properties of 1−3 in Acetonitrile at Room Temperature[a]

compound	λ_L/nm	Φ_L[b]	τ_L[c]/μs	k_q/M^{-1} s^{-1}	Φ_Δ[d]
1	685	0.70	320	1.9×10^8	0.66
2	685	0.93	320	1.9×10^8	0.71
3	685	0.77	330	2.0×10^8	0.67

[a] λ_L is the maximum of the luminescence emission band, Φ_L is the quantum yield of luminescence (measured in oxygen-free acetonitrile), τ_L is the lifetime of the triplet states in oxygen-free acetonitrile, k_q is the bimolecular rate constant for the quenching of the triplet states by oxygen, and Φ_Δ is the quantum yield of singlet oxygen formation in oxygen-saturated acetonitrile. [b] Estimated error is 10%, excited at 440 nm. [c] Estimated error is 10%, excited at 390 nm. [d] Estimated error is 10%, excited at 308 nm.

Time-resolved luminescence and transient measurements were performed to characterize the behavior of the excited states. All cluster complexes had detectable transient absorptions in acetonitrile within the range of 450 to 600 nm (Figure S43 in the Supporting Information). The luminescence traces, which are attributed to the emission from the triplet states by analogy with $[Mo_6Cl_{14}]^{2-}$,[26] were quenched by oxygen with the same rate constants as the transient absorptions (Figure S44 in the Supporting Information). The agreement between these two measurements confirms that the observed transient absorptions belong to the transitions from the same electronic states as the luminescence emissions.

The luminescence decay times of **1**−**3** were 320−330 μs. The Φ_L values, obtained for **1**, **2**, and **3**, are 0.70, 0.93 and 0.77, respectively, and apart from $[Mo_6I_8(OOCCF_3)_6]^{2-}$,[1] these values are the highest reported for the molybdenum cluster complexes. The intensity of red luminescence was strongly quenched in the presence of oxygen with bimolecular rate constants on the order of 10^8 M^{-1} s^{-1}. The investigation of the production of $O_2(^1\Delta_g)$ was performed by the measurement of its luminescence with a band maximum at approximately 1270 nm. The quantum yields Φ_Δ of 0.66, 0.71, and 0.67 for **1**, **2**, and **3**, respectively, are similar to the values reported for the $[Mo_6L_{14}]^{2-}$ complexes.[3] The only notable difference among the prepared complexes is a higher Φ_L for **2**; however, there is no evident correlation between the photophysical properties of **1**−**3** and the acidities of *closo*-dicarbaborane C-carboxylic acids (pK_a(1-HOOC-1,2-closo-$C_2B_{10}H_{11}$) = 13.9, pK_a(1-HOOC-1,7-closo-$C_2B_{10}H_{11}$) = 16.2, pK_a(1-HOOC-1,12-closo-$C_2B_{10}H_{11}$) = 16.7 in acetonitrile).[22] Overall, compounds **1**−**3** displayed luminescence properties similar to those of $(n\text{-}Bu_4N)_2[Mo_6I_8(OOCCF_3)_6]$[1] or $(n\text{-}Bu_4N)_2[Mo_6I_8(OOCC_3F_7)_6]$.[7]

Preparation and Characterization of Water Dispersions. The luminescent hydrogel particles, **2@poly-β-CD**, were prepared by self-assembly of β-cyclodextrin polymer and **2** in a water/THF mixture (1:1, v/v), followed by the evaporation of THF. The concentrations of **2** were 3.6×10^{-5} M and the estimated molar ratio of β-cyclodextrin/**2** was 7.4. Compound **2** was chosen for further investigation since it has the highest luminescence efficiency among the prepared complexes. A water dispersion of **2**, prepared in a similar fashion as **2@poly-β-CD**, was also investigated for comparative purposes.

The water dispersions of **2** and **2@poly-β-CD** did not sediment, even after several weeks at room temperature. Figure 3 shows the evolution of the average hydrodynamic diameters

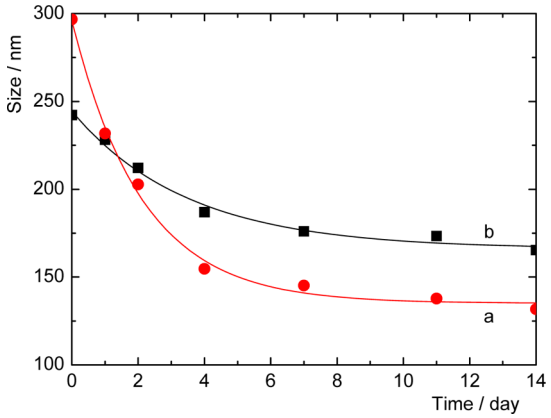

Figure 3. Time evolution of the particle size distribution of **2** (a) and **2@poly-β-CD** (b) in water at room temperature.

(Z-average) measured by dynamic light scattering (see also Figure S45 in the Supporting Information). In the absence of the β-cyclodextrin polymer, compound **2** formed aggregates of a 300 nm diameter with a narrow size distribution (polydispersity index, PDI, was 0.035). The aggregate size progressively decreased with time (145 nm, PDI = 0.071 after 7 days and 132 nm, PDI = 0.042 after 14 days). The formation of aggregates of molybdenum cluster complexes in water has been already reported; however, in that case, aggregates were formed via the hydrolysis of $Cs_2[Mo_6Br_{14}]$ and particles were of a significantly larger diameter (in the micrometer range).[11] The **2@poly-β-CD** particles displayed an initial diameter of 242 nm with a narrow size distribution (PDI = 0.087). The size reached 165 nm (PDI = 0.088) after 14 days and did not show any subsequent variations. The decrease in the diameter reflects structural rearrangement of the dispersed particles and in terms of luminescence properties it reduces the scattering of light.

The HRTEM and AFM observations of **2@poly-β-CD** particles are shown in Figure 4 and Figure 5, respectively. The deposited particles had an ovoidal shape with the size along the major axis to be approximately 250 nm and along the minor axis to be approximately 150 nm. The AFM images showed the thicknesses to be approximately 90 nm. These data are in accordance with the particle hydrodynamic diameters in dispersions measured by dynamic light scattering (~160 nm). The mapping of molybdenum and iodine atoms via energy-

dx.doi.org/10.1021/ic502144z | Inorg. Chem. 2014, 53, 13012−13018

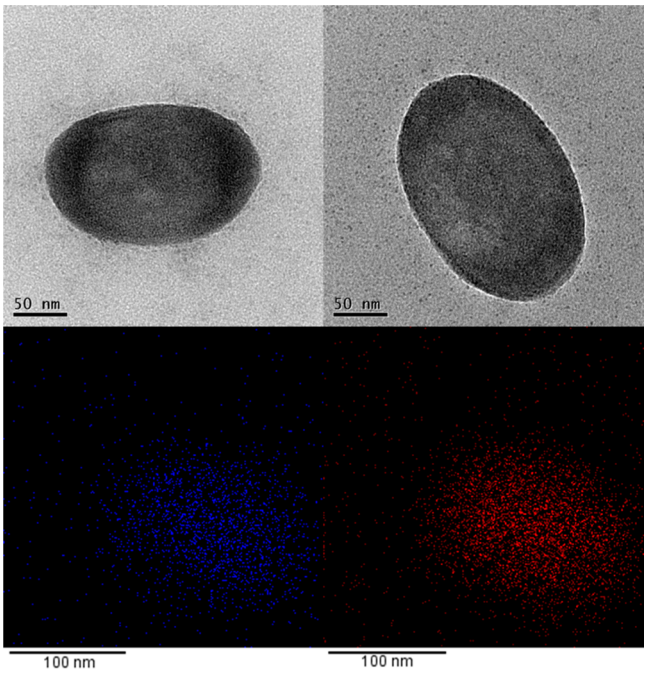

Figure 4. Particles of **2@poly-β-CD**: TEM images of independent particles (top), mapping of molybdenum (blue) and iodine (red) atoms via energy-dispersive X-ray spectroscopy (bottom).

dispersive X-ray spectroscopy indicated that the molecules of **2** are distributed homogeneously in the volume of the particles.

The formation of cyclodextrin adducts with carborane derivatives with association constants on the order of 10^3–10^4 M^{-1} has already been reported.[19,20] The most relevant method for characterization of such interactions is ^{1}H NMR spectroscopy. This method was not successful in the case of the hydrogel particles because of the insolubility of **2** in water and very broad peaks of relevant cyclodextrin protons in D_2O.[27] The inclusion of the apical carborane ligands in the β-cyclodextrin cavities in **2@poly-β-CD** was thus investigated by FTIR spectroscopy. As shown in Figure S46 (in the Supporting Information), the C–H stretching band of **2@poly-β-CD** exhibited a shoulder at 2955 cm^{-1}, which was not present in the physical mixture. The attenuation of the B–H band intensity in **2@poly-β-CD** when compared with the physical mixture is indicative of the formation of an inclusion complex resulting in a shielding of the host ligands.[28] There is no evidence that the molar ratio of β-cyclodextrin/**2** used of approximately 7.4 provided capping of all carborane ligands; however, the results showed that this ratio is enough to make the hydrolysis of the cluster complex a marginal process (see below).

Photophysical Properties of Water Dispersions. Figure 6 shows the normalized luminescence spectra of prepared

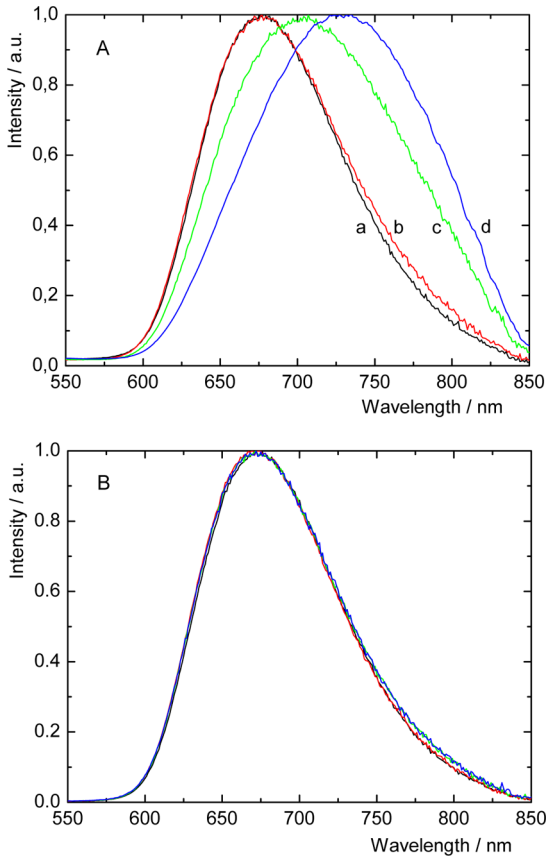

Figure 6. Normalized emission spectra: (A) **2** in water after the preparation (a) and 1 day (b), 4 days (c), and 14 days (d) after the preparation. (B) **2@poly-β-CD** measured after the preparation and following 14 days (the same color code as in (A)). Excited at 440 nm.

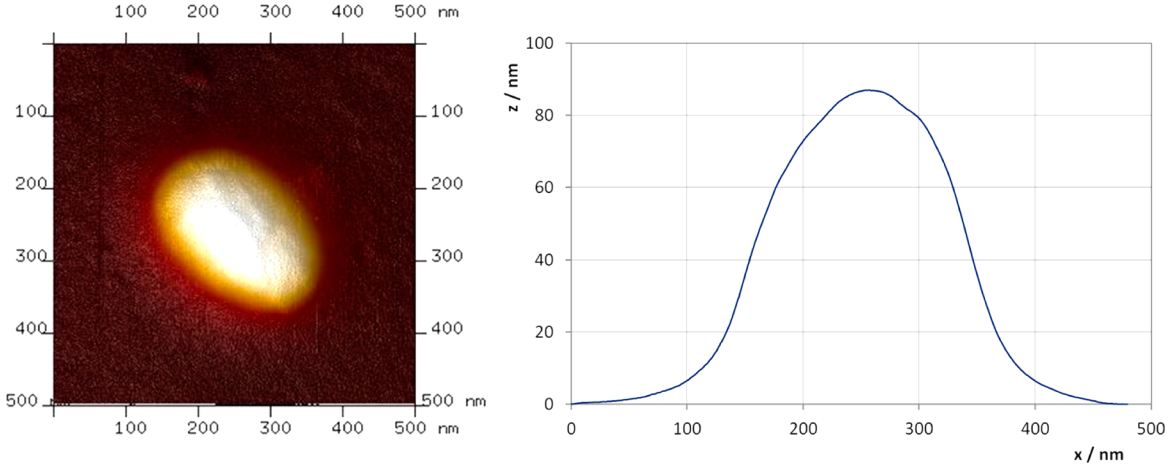

Figure 5. Particle of **2@poly-β-CD**: AFM image with the corresponding profile analysis.

dx.doi.org/10.1021/ic502144z | Inorg. Chem. 2014, 53, 13012–13018

particles at various times after the preparation. The freshly prepared dispersions of **2** and **2@poly-β-CD** displayed identical luminescence spectra, indicating that interactions between the apical ligands and cyclodextrins did not affect the energies of the cluster radiative transitions. The maxima were located at 675 nm and blue-shifted by 10 nm when compared with the luminescence spectra of **2** in acetonitrile. The shift can be attributed to the higher polarity of water compared to that of acetonitrile.

A progressive red shift of the luminescence maximum of water dispersions of **2** to 730 nm after 14 days indicated a continuous cluster hydrolysis. Indeed, the ESI-MS analyses of aged H_2O/acetonitrile solutions of **2** revealed the replacement of an apical ligand by a hydroxyl ligand to form $[Mo_6I_8(1\text{-}OOC\text{-}1,7\text{-}closo\text{-}C_2B_{10}H_{11})_5(OH)]^{2-}$ (Figure S47 in the Supporting Information). In contrast, the features of the luminescence spectra of **2@poly-β-CD** remained unchanged even after 14 days of aging. When the molar ratio β-cyclodextrin/**2** was approximately 1, complex **2** hydrolyzed in a similar manner as that observed with water dispersions of **2** (Figure S48 in the Supporting Information). These results illustrate the crucial role of β-cyclodextrins in the protection of **2** against hydrolysis.

As shown in Figure 7, the luminescence of **2@poly-β-CD** was efficiently quenched in the presence of oxygen. Time-resolved luminescence spectroscopy revealed that luminescence decays can be best analyzed by a two-exponential model in both air-saturated solutions and in oxygen-free solutions (Table 2). Despite the decrease in the particle size of **2@poly-β-CD** over time, the respective emission lifetimes and their contributions did not change within the studied period of 14 days. In contrast, the luminescence lifetimes of the fresh water dispersions of **2** were significantly shorter, and the contribution of a short-lived component considerably increased over time. These variations can be ascribed to the increasing contribution of hydrolyzed products having different emission spectra and lifetimes than the starting complex. The discrepancy between the initial lifetimes of **2** and **2@poly-β-CD** can be attributed to different environments around the luminescent molecules that affect the rate constants of the radiative transitions.

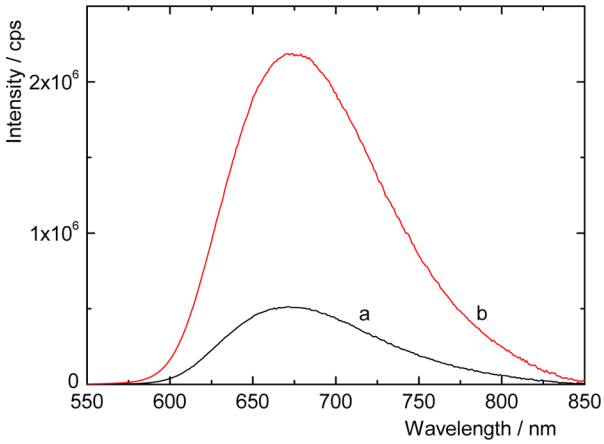

Figure 7. Emission spectra of **2@poly-β-CD** in water saturated by air (a) and in the absence of oxygen (b). Excited at 440 nm.

Table 2. Photophysical Properties of Particles of 2 and 2@poly-β-CD in Water at Room Temperature[a]

particles	λ_L/nm	τ_L[b]/μs (air)	τ_L[b]/μs (oxygen-free)
2[c]	675	7(29%), 30(71%)	-
2[d]	730	8(46%), 37(54%)	18(40%), 101(60%)
2@poly-β-CD	675	19(27%), 47(73%)	85(23%), 173(77%)

[a] λ_L is the maximum of the emission band, τ_L are the lifetimes of the triplet states in air-saturated and oxygen-free water. The pairs of lifetimes and their contributions were obtained by biexponential fits. [b] Estimated error is 10%, excited at 390 nm. [c] Fresh dispersion. [d] Dispersion after 14 days.

The quenching of **2@poly-β-CD** luminescence in air suggested that the cluster molecules in the hydrogel particles are accessible to dissolved oxygen. Assuming radial diffusion over some time period,[29] t, then the distance traveled by oxygen can be expressed as $d = (6tD)^{1/2}$ where D is the diffusion coefficient of oxygen in polysaccharide hydrogels ($D \sim 2 \times 10^{-5}$ cm^2 s^{-1})[30] that is comparable to that in water. Then, during the lifetime of the triplet states (Table 2) the oxygen molecule can diffuse over 680 nm that is much more than the particle size. From this comparison it follows that the local concentrations of oxygen in the particles compared to that of the cluster do not interfere with the quenching of the cluster luminescence.

The quenching of **2@poly-β-CD** luminescence by oxygen also indicated the ability of **2** to produce $O_2(^1\Delta_g)$. Direct evidence of the production of $O_2(^1\Delta_g)$ was obtained by measuring its typical luminescence at 1275 nm (Figure S49 in the Supporting Information). The size of the hydrogel particles is critical for diffusion of $O_2(^1\Delta_g)$ outside the particles because its lifetime in aqueous media is in the μs region (e.g., the lifetime of $O_2(^1\Delta_g)$ in pure water is ~3.5 μs).[31] Using similar reasoning to that above, a molecule of $O_2(^1\Delta_g)$ can diffuse over mean radial distances of at least 200 nm during its lifetime. These results show that $O_2(^1\Delta_g)$ can diffuse outside the hydrogel particles making them good carriers of these sensitizers for the photooxidation of target molecules/objects in aqueous media.

CONCLUSION

We prepared a series of three new molybdenum cluster complexes by grafting icosahedral *closo*-dicarbaborane C-carboxylates to a $\{Mo_6I_8\}^{4+}$ core. These complexes had a red luminescence with high quantum yields and were self-assembled with β-cyclodextrin polymer to form hydrogel particles without any chemical modification of the complex. The hydrogel particles showed a monodisperse distribution and their hydrodynamic diameter varied from 240 nm following preparation to 160 nm after 14 days, at which time it maintained a constant value. These particles containing dispersed **2** were luminescent and the emission maxima and lifetime were unchanged within 14 days of aging because of the protecting effect of the β-cyclodextrin cavities against hydrolysis. This effect is explained by host−guest interactions between carborane apical ligands and the β-cyclodextrin cavities. In contrast, a red shift of the luminescence observed for the dispersions of **2** was indicative of the cluster hydrolysis. The invariance of the photophysical properties of the hydrogel particles coupled with the oxygen sensitivity of the luminescence are attractive features for long-term biological experiments involving optical oxygen probing by phosphorescence-lifetime imaging microscopy. The embedded cluster complexes act as efficient singlet oxygen sensitizers and the high content of boron atoms (60 per complex) make the

dx.doi.org/10.1021/ic502144z | Inorg. Chem. 2014, 53, 13012−13018

hydrogel particles potentially useful as dual agents for photodynamic therapy/boron neutron capture therapy. From a prospective point of view, the usage of polymeric cyclodextrins is advantageous as it allows for postfunctionalization of the surface of the hydrogel particles for the targeting of specific receptors of tumor cells.[18] Further investigations are planned to evaluate the toxicity of this new material and its potential in biological applications.

■ ASSOCIATED CONTENT

Supporting Information

NMR chemical shifts of icosahedral *closo*-dicarbaborane C-carboxylic acids, ^{11}B and ^{1}H NMR spectra of **1**, **2**, and **3**, mass spectra, transient absorption spectra, luminescence spectra, size distribution of particles, and FTIR spectra. This material is available free of charge via the Internet at http://pubs.acs.org.

■ AUTHOR INFORMATION

Corresponding Authors

*E-mail: kaplan@iic.cas.cz, Tel.: +(420) 266 172 194.
*E-mail: lang@iic.cas.cz, Tel.: +(420) 266 172 193.

Notes

The authors declare no competing financial interest.

■ ACKNOWLEDGMENTS

This work was supported by the Czech Science Foundation (No. 13-05114S).

■ REFERENCES

(1) Kirakci, K.; Kubát, P.; Dušek, M.; Fejfarová, K.; Šícha, V.; Mosinger, J.; Lang, K. *Eur. J. Inorg. Chem.* **2012**, *2012*, 3107−3111.
(2) Jackson, J. A.; Turro, C.; Newsham, M. D.; Nocera, D. G. *J. Phys. Chem.* **1990**, *94*, 4500−4507.
(3) Kirakci, K.; Kubát, P.; Langmaier, J.; Polívka, T.; Fuciman, M.; Fejfarová, K.; Lang, K. *Dalton Trans.* **2013**, *42*, 7224−7232.
(4) Ghosh, R. N.; Baker, G. L.; Ruud, C.; Nocera, D. G. *Appl. Phys. Lett.* **1999**, *75*, 2885−2887.
(5) Zhao, Y.; Lunt, R. R. *Adv. Energy Mater.* **2013**, *3*, 1143−1148.
(6) Kumar, P.; Kumar, S.; Cordier, S.; Paofai, S.; Boukherroub, R.; Jain, S. L. *RSC Adv.* **2014**, *4*, 10420−10423.
(7) Sokolov, M. N.; Mihailov, M. A.; Peresypkina, E. V.; Brylev, K. A.; Kitamura, N.; Fedin, V. P. *Dalton Trans.* **2011**, *40*, 6375−6377.
(8) Molard, Y.; Dorson, F.; Cîrcu, V.; Roisnel, T.; Artzner, F. *Angew. Chem., Int. Ed.* **2010**, *49*, 3351−3355.
(9) Kirakci, K.; Fejfarová, K.; Kučeráková, M.; Lang, K. *Eur. J. Inorg. Chem.* **2014**, *2014*, 2331−2336.
(10) Molard, Y.; Labbé, C.; Cardin, J.; Cordier, S. *Adv. Funct. Mater.* **2013**, *23*, 4821−4825.
(11) Aubert, T.; Burel, A.; Esnault, M.-A.; Cordier, S.; Grasset, F.; Cabello-Hurtado, F. *J. Hazard. Mater.* **2012**, *219*, 111−118.
(12) Aubert, T.; Cabello-Hurtado, F.; Esnault, M.-A.; Neaime, C.; Lebret-Chauvel, D.; Jeanne, S.; Pellen, P.; Roiland, C.; Le Polles, L.; Saito, N.; Kimoto, K.; Haneda, H.; Ohashi, N.; Grasset, F.; Cordier, S. *J. Phys. Chem. C* **2013**, *117*, 20154−20163.
(13) Efremova, O. A.; Shestopalov, M. A.; Chirtsova, N. A.; Smolentsev, A. I.; Mironov, Y. V.; Kitamura, N.; Brylev, K. A.; Sutherland, A. J. *Dalton Trans.* **2014**, *43*, 6021−6025.
(14) Martin Del Valle, E. M. *Proc. Biochem.* **2004**, *39*, 1033−1046.
(15) Loftsson, T.; Brewster, M. E. *J. Pharm. Sci.* **1996**, *85*, 1017−1025.
(16) Aoyama, Y.; Otsuki, J.; Nagai, Y.; Kobayashi, K.; Toi, H. *Tetrahedron. Lett.* **1992**, *33*, 3775−3778.
(17) Wintgens, V.; Layre, A.-M.; Hourdet, D.; Amiel, C. *Biomacromolecules* **2012**, *13*, 528−534.
(18) Yan, H.; He, L.; Ma, C.; Li, J.; Yang, J.; Yang, R.; Tan, W. *Chem. Commun.* **2014**, *50*, 8398−8401.
(19) Vaitkus, R.; Sjöberg, S. *J. Incl. Phenom. Macrocycl. Chem.* **2011**, *69*, 393−395.
(20) Ohta, K.; Konno, S.; Endo, Y. *Tetrahedron Lett.* **2008**, *49*, 6525−6528.
(21) Ching, H. Y. V.; Clifford, S.; Bhadbhade, M.; Clarke, R. J.; Rendina, L. M. *Chem.—Eur. J.* **2012**, *18*, 14413−14425.
(22) Grimes, R. N. *Carboranes*, 2nd ed.; Elsevier Inc.: Amsterdam, 2011.
(23) Grafstein, D.; Cohen, M. S.; Fein, M. M.; Dvorak, J.; Schwartz, N.; Smith, H.; Bobinski, J. *Inorg. Chem.* **1963**, *2*, 1120−1125.
(24) Franco, C.; Olmsted, J. *Talanta* **1990**, *37*, 905−909.
(25) Tanaka, F.; Furuta, T.; Okamoto, M.; Hirayama, S. *Phys. Chem. Chem. Phys.* **2004**, *6*, 1219−1226.
(26) Miki, H.; Ikeyama, T.; Sasaki, Y.; Azumi, T. *J. Phys. Chem.* **1992**, *96*, 3236−3239.
(27) Zhang, W.; Gong, X.; Liu, C.; Piao, Y.; Sun, Y.; Diao, G. *J. Mater. Chem. B* **2014**, *2*, 5107−5115.
(28) Crupi, V.; Majolino, D.; Venuti, V.; Guella, G.; Mancini, I.; Rossi, B.; Verrocchio, P.; Viliani, G.; Stancanelli, R. *J. Phys. Chem. A* **2010**, *114*, 6811−6817.
(29) Yan, F.; Kopelman, R. *Photochem. Photobiol.* **2003**, *78*, 587−591.
(30) Li, R. H.; Altreuter, D. H.; Gentile, F. T. *Biotechnol. Bioeng.* **1996**, *50*, 365−373.
(31) Wilkinson, F.; Helman, W. P.; Ross, A. B. *J. Phys. Chem. Ref. Data* **1995**, *24*, 663−1021.